Charge Transfer Excited-State Dynamics in DNA Duplexes Substituted with an Ethynylpyrenyldeoxyuridine Electron Source and a Fluorodeoxyuridine Electron Trap

Samir T. Gaballah,† Galen Collier, and Thomas L. Netzel*

Department of Chemistry, Georgia State University, P.O. Box 4098, Atlanta, Georgia 30332-4098

Received: December 6, 2004; In Final Form: March 24, 2005

Studies of six 5-(pyren-1-yl-ethynyl)-2′-deoxyuridine (U^{PY})-substituted DNA duplexes in this work test and support the conclusions reported by Gaballah et al. (*J. Phys. Chem. B* **2005**, *109*, 5927−5934) based on investigations of 5-(2-pyren-1-yl-ethylenyl)-2′-deoxyuridine (U^{PE})-substituted DNA hairpins. As expected because of the rigid ethynyl linker in U^{PY} (compared to the flexible ethylenyl linker in U^{PE}), U^{PY}-substituted duplexes do not show enhanced charge transfer (CT) emission quantum yields for duplexes with 5-fluorodeoxyuridine (U^{F}) electron traps near U^{PY} compared to duplexes without traps. Furthermore, the average CT lifetime and emission quantum yield of U^{PY}-substituted duplexes is independent of the U^{F} trap location. These new results strongly suggest that the excess electron in the $PY^{\bullet+}/dU^{\bullet-}$ CT state of U^{PY} is restrained from hopping to nearby U^{F} traps due to attraction to $PY^{\bullet+}$.

Introduction

Excess electron transfer (ET) or transport in DNA can potentially occur if a covalently attached electron donor is photoexcited and transfers one of its electrons into the DNA base stack. While the areas of oxidative hole transfer and hopping in DNA have been well investigated,[1,2] many aspects of excess electron transfer in DNA are still not understood. Important initial investigations in this area used pulse radiolysis to add an excess electron to DNA.[3−8] However recently, apparently contradictory results have been reported for excess electron-transfer reactions in DNA, but the apparent discrepancies could result from the different means of excess electron generation and observation.[9−12] So far photochemical studies of excess electron injection and transport in DNA have employed flavin,[11,13−16] stilbenediether,[17−19] 1,5-diaminonaphthalene,[10,20] pyrene,[21−25] and ketyl radical anions[9] as electron sources.

A number of spectroscopic studies of pyrenyl-deoxyuridine (dU) nucleoside conjugates[26−29] have shown that photoexcitation of the pyrenyl chromophore in these conjugates in a polar solvent initially forms the local pyrenyl $^1(\pi,\pi^*)$ excited state, but that this state in turn rapidly undergoes intramolecular ET to form the $pyrene^{\bullet+}/dU^{\bullet-}$ charge-separated (CS) product. Both of these states emit, but the pyrenyl $^1(\pi,\pi^*)$ state emits at higher energy than the $pyrene^{\bullet+}/dU^{\bullet-}$ CS product and has three distinct carbon−carbon stretching vibrational bands. The emission spectrum of the $pyrene^{\bullet+}/dU^{\bullet-}$ CS (or charge transfer, CT) product, in contrast, is broad and structureless, overlapping the pyrenyl $^1(\pi,\pi^*)$ emission region and extending well beyond it to a longer wavelength. Wagenknecht, Fiebig, and co-workers produced DNA duplexes substituted with two kinds of pyrene−dU nucleotide conjugates.[21−24] One type of pyrenyl nucleotide was based on the 5-(pyren-1-yl)-2′deoxyuridine (PdU) nucleoside originally prepared and studied by Netzel, Eaton, and co-workers.[30,31] In PdU, the pyrenyl and uracil subunits were directly bonded together. The second type of pyrenyl nucleotide conjugate was based on the 5-(pyren-1-yl-ethynyl)-2′-deoxyuridine nucleoside (PYdU) originally prepared by Korshun and co-workers.[32] In PYdU, the pyrenyl and uracil subunits were joined by an ethynyl linker.

In a recent work by Gaballah et al.,[25] pyrenyl-substituted DNA hairpins (HPs) were studied to observe their $pyrene^{\bullet+}/dU^{\bullet-}$ CT excited-state dynamics. All of the HPs had a central tetra-T loop and a single 5-(2-pyren-1-yl-ethylenyl)-2′-deoxyuridine (U^{PE}) substitution in the central region of their stems. Several of the HPs were also substituted with 5-XdU excess electron traps (U^{X}), where X = Br or F, to learn about the effects of these traps on $pyrene^{\bullet+}/dU^{\bullet-}$ CT excited-state dynamics. For ease of discussion, charge separation (CS) and recombination (CR) processes that occurred within the pyrenyl-substituted nucleotide were termed type 1, while those that occurred between pyrene and pyrimidines external to the pyrenyl-substituted nucleotide were termed type 2. In this HP work, five HPs lacking U^{X} traps showed an average CT lifetime of 1.06 ± 0.15 ns whether same-strand Ts adjacent to the U^{PE} electron source were present in both the 5′- and 3′-directions, present only in the 5′-direction, or even absent in both directions. In contrast, however, all three HPs with U^{X} electron traps on the same strand as U^{PE} had both an average CT lifetime in the 2.1−2.5 ns range and an "enhanced" CT emission quantum yield (i.e., emission in excess of that expected based on comparison of average CT lifetimes). The combination of these two differences for all HPs with U^{X} traps compared to all HPs lacking such traps strongly suggested that type 2 CS electron injection was occurring in U^{PE}-labeled HPs in addition to type 1 CS injection within U^{PE} itself. This conclusion was further supported by the increase in the pyrenyl $^1(\pi,\pi^*)$ emission features and in the total emission quantum yield that was seen as same-strand Ts flanking U^{PE} were switched to the opposite strand. The enhanced CT emission quantum yield in HPs with U^{X} electron traps compared to HPs lacking traps resulted from type 2 CS injected electrons migrating to uracil in U^{PE} (i.e., $PE^{\bullet+}/dU$) and thus indirectly forming the emissive $PE^{\bullet+}/dU^{\bullet-}$

* Author to whom correspondence should be addressed. E-mail: tnetzel@gsu.edu.

† Present address: Photochemistry Department, National Research Center, El Tahrir Street, Dokki, Cairo, Egypt.

10.1021/jp044457x CCC: $30.25
Published on Web 05/28/2005

CHART 1: Structural Drawings of the U^{PY} and U^{F} Nucleotides Incorporated into the DNA Duplexes Studied Here[a]

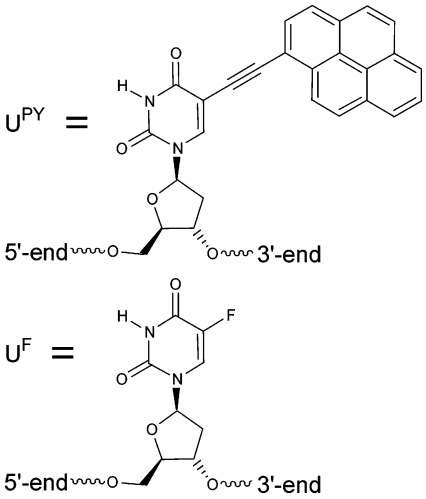

[a] The nucleosides are termed, respectively, PYdU and FdU.

TABLE 1: Duplex Base Sequence, Melting Temperature (T_m), Molar Absorbance (ϵ_{259}), and Emission Quantum Yield (Φ_{em})

duplex	base sequence[a]	T_m[b] (°C)	$\epsilon_{259} \times 10^{-5}$ [c] (M^{-1} cm^{-1})	Φ_{em}[d]
1	GGTTTTU^{F}**U^{PY}**AAAGG	39.3 ± 0.7	2.51	0.020
2	GGTTTU^{F}T**U^{PY}**AAAGG	39.7 ± 0.7	2.28	0.016
3	GGTTU^{F}TT**U^{PY}**AAAGG	39.9 ± 0.8	2.45	0.022
4	GGTU^{F}TTT**U^{PY}**AAAGG	40.6 ± 0.8	2.37	0.021
5	GGATAA**U^{PY}**AATAGG	37.1 ± 0.5	2.61	0.017
6	GGAATT**U^{PY}**TTAAGG	40.0 ± 0.5	2.28	0.032

[a] 5′→3′ base sequence. [b] Duplex concentrations for T_m measurements were 3.4−3.8 × 10^{-6} M in 7.5 mM phosphate buffer with 10 μM Na_2EDTA and 1.0 M NaCl. [c] Error is ±3%. [d] Emission quantum yields were measured relative to PBA in deaerated MeOH with Φ_{em} equal to 0.065; Φ_{em} error is ±10%.

CT state of U^{PE}. This latter conclusion appeared reasonable as Coulombic attraction favored excess electron hopping from stem traps and bases toward $PE^{\bullet+}$/dU. Although this study presented compelling circumstantial evidence to support its conclusions, additional studies in this area are still warranted to cement its conclusions.

In this work, six DNA duplexes are studied at 10 °C to observe $PY^{\bullet+}/dU^{\bullet-}$ CT excited-state dynamics in them following photoexcitation at 355 nm.[33] All are 13 base pairs long and have a central ethynylpyrenyl U^{PY} nucleotide. Importantly, four of these duplexes are also substituted near U^{PY} in the 5′-direction with a same-strand U^{F} nucleotide to serve as an excess electron trap. (See Chart 1 for structural drawings of the U^{PY} and U^{F} nucleotides and Table 1 for DNA duplex base sequences.) Some idea of the relative effect on the uracil reduction potential due to changing a C5-methyl group to a fluorine can be estimated by noting that in the case of flavin mononucleotide (FMN) the $2e^-$ reduction potential of FMN_{ox}/1,5-dihydro-$FMN_{red}H_2$ varies due to substitution at position 8, respectively, as −208 (Me), −167 (F), and −148 (Br) versus the standard hydrogen electrode.[34] Thus, the U^{F} and U^{Br} nucleotides are likely to be 40−50 mV easier to reduce than T. In agreement with these considerations, the work by Gaballah et al.[25] showed that 5′-adjacent U^{F} and U^{Br} traps were more effective oxidative quenchers of the local pyrenyl $^1(\pi,\pi^*)$ state of U^{PE} than a 5′-adjacent T. Additionally, both U^{F} and U^{Br} were shown to be shallow electron traps as excess electrons on them migrated to uracil in U^{PE} (i.e., $PE^{\bullet+}$/dU) to form the emissive $PE^{\bullet+}/dU^{\bullet-}$ CT state of U^{PE}. The U^{PY}-substituted duplexes in this work provide a test of the conclusions reported by Gaballah et al.[25] based on studies of U^{PE}-substituted HPs. Because the ethynyl linker in U^{PY} is more rigid than the ethylenyl linker in U^{PE} and type 1 photoinduced CS may be faster in a larger fraction of conformers of U^{PY} than in U^{PE}, most if not all of the type 2 CS found in the earlier study should be eliminated in U^{PY}-substituted duplexes.[35] Additionally, if the excess electron in the $PY^{\bullet+}/dU^{\bullet-}$ CS product of U^{PY} is restrained from hopping to nearby U^{F} traps due to attraction to $PY^{\bullet+}$, the CT emission quantum yield and average lifetime of U^{PY}-substituted duplexes should be independent of trap location and much the same whether or not they are substituted with U^{F} traps. A final topic addressed here is how do the $PY^{\bullet+}/dU^{\bullet-}$ CT excited-state dynamics of intact duplexes compare to those of melted duplexes.

Experimental Materials and Methods

Materials. Supplies for FPLC DNA purification and spectroscopy were purchased from the following vendors and used as received: pyrenebutanoic acid (PBA, high-purity grade) from Molecular Probes and methanol (MeOH) and acetonitrile (MeCN) from Burdick & Jackson (either spectroscopic or HPLC grade).

UV−Vis and Circular Dichroism (CD) Absorbance. UV−vis absorbance spectra were recorded on a Shimadzu UV-2501PC high-performance spectrophotometer equipped with a double monochromator to reduce stray light. Absorbance spectra were recorded every 0.5 nm with a spectral bandwidth (SBW) of 1 nm using quartz cells with a path length of 1 cm. CD absorbance spectra were recorded on a JASCO-810 spectropolarimeter using a SBW of 1 nm and self-masking quartz semimicrocells. Absorbances of DNA solutions at 260 nm were adjusted to 0.8−0.9. CD spectra were recorded at 10.0 ± 0.2 °C in the 205−400 nm range. The CD spectra of identical buffer solutions lacking DNA duplexes were used to correct the baseline of the CD spectra of the DNA solutions. Figure 1S of the Supporting Information presents overlayed plots of circular dichroism spectra ($\Delta\epsilon$) for the six duplexes in this study. All show characteristic B-DNA CD signatures.

Fluorescence Spectra and Quantum Yield Measurements. For steady-state fluorescence spectra (and as well for fluorescence lifetime studies, below), quartz fluorescence cuvettes with screw-open caps and Teflon−silicone septa (Wilmad Glass, WG-9F/OC-Q-10) were used. All fluorescence samples were deoxygenated prior to spectral or kinetics measurements by bubbling with N_2 gas for 40 min while stirring.

Fluorescence spectra were recorded on a PTI QuantaMaster spectrofluorometer using 4-nm excitation and 2-nm emission SBWs. Spectra were recorded at 10.0 ± 0.2 °C from 350 to 625 nm at 0.5-nm intervals using a 2-s integration time at each wavelength and smoothed over 10-nm intervals. Samples were excited at either 341 or 365 nm in a quartz 1-cm fluorescence cuvette using right-angle excitation and emission geometry. Polarization artifacts were avoided by positioning a vertical polarizer immediately in front of the sample in the excitation beam and recording emission spectra through a second polarizer adjusted to 54.7° with respect to the vertical ("magic angle").[36] All spectra were corrected for the wavelength-dependent emission sensitivity of the spectrofluorometer (W/cm^2) using correction factors developed at Georgia State University. A detailed description of our procedure for measuring absolute emission quantum yields (Φ_{em}) is provided in the Supporting Information.

Picosecond Fluorescence Lifetime Measurements. Fluorescence lifetime measurements were carried out using third harmonic pulses (355 nm) from a custom-built picosecond-laser flash-photolysis system as the excitation source.[37,38] In this system, an active−passive, mode-locked, Q-switched Nd^{3+}/YAG laser (Continuum, Inc.) was operated at 15 Hz to produce single excitation pulses of ~35 μJ of energy with durations of ca. 25 ps (full width at half-maximum). The excitation beam was collimated to 3 mm in diameter at the emission cell and passed through a Glan-Thompson laser polarizer set to the vertical prior to entering the sample cell. The excitation and emission beams were oriented at 90° with respect to each other. Emission was detected through a second Glan-Thompson polarizer set at 54.7° with respect to the vertical and was resolved by a double monochromator (Instruments SA, model DH10) in additive dispersion; 2-mm slits were used producing an 8-nm SBW. The monochromator's output was detected by a Hamamatsu R1564U microchannel plate (MCP, 200-ps rise time). The detector's response was recorded by a Tektronix SCD1000 transient digitizer (≤0.35-ns rise time calculated from the bandwidth, ≤120-ps rise time for a step input 0.5 times the vertical range). Each transient measurement, whether of a sample's emission decay, the instrument response to scattered laser light, or the detector's background, was recorded as a 500-point average of 1000 laser firings.

Emission transient curves were downloaded from the Tektronix SCD1000 digitizer to a PC and analyzed with software from Photon Technology. This software deconvoluted the detector's instrument response to yield exponential lifetime fits to the emission decay data. An aqueous solution of glycogen provided the scattered light for the instrument response function. Additional experimental details are given in the Supporting Information, and a full description of the lifetime fitting procedure used in this study has been presented by Netzel et al.[31] Table 2 provides errors for emission lifetimes averaged over all decay components and multiple wavelengths. Table 1S of the Supporting Information presents emission kinetics data at nine wavelengths for duplexes **1**−**6** at 10 °C and at six wavelengths for duplexes **4**−**6** at 70 °C.

DNA Synthesis. Six 13-mer DNA single strands (Table 1) were synthesized at the Parker H. Petit Institute for Bioengineering and Bioscience at the Georgia Institute of Technology using a U^{PY} β-cyanoethylphosphoramidite synthesized at Georgia State University and a U^{F} β-cyanoethylphosphoramidite purchased from Glen Research. (See Chart 1 for structures of the U^{PY} and U^{F} nucleotides incorporated into the 13-mer strands.) Standard solid-phase DNA synthetic protocols were followed using a commercial DNA synthesizer. Complementary 13-mer single strands were purchased from Qiagen. All strands were synthesized in 1-μmol batches. Lyophilized strands were dissolved in a polytetrafluoroethylene vial in 1 mL of deionized water from a Millipore Milli-Q system (18.0 MΩ), wrapped in aluminum foil, and stored in a freezer for future use. Detailed descriptions of our DNA purification and desalting procedures are presented in the Supporting Information.

DNA Single-Strand Analysis. Mass spectra were run on all oligomers at the Georgia Institute of Technology using electrospray ionization. All masses found were within 0.6 amu of the calculated mass. Single-strand melting experiments were run at 260 nm between 5 and 90 °C on all oligomers in deionized water using absorbance semi-microcells with a 1-cm optical path length (A_{260} = 0.8) to see if the strands aggregated at low temperatures. None did, as all T_m measurements yielded linear absorbance versus temperature plots.

TABLE 2: Kinetics Data for Duplexes 1−6 at 10 °C and 4−6 at 70 °C Averaged over the Indicated Wavelength Ranges[a,b]

duplex	$\langle\tau_1\rangle$ (ns) (A_1)	$\langle\tau_2\rangle$ (ns) (A_2)	$\langle\tau_3\rangle$ (ns) (A_3)	$\langle\tau\rangle$ (ns)[c]
	410−600 Emission at 10 °C			
1	0.51 (0.40)	1.47 (0.58)	4.23 (0.02)	1.14
2	0.28 (0.32)	1.19 (0.56)	3.12 (0.12)	1.13
3	0.33 (0.23)	1.24 (0.70)	3.91 (0.07)	1.23
4	0.37 (0.30)	1.35 (0.57)	3.63 (0.13)	1.37
5	0.65 (0.40)	1.35 (0.52)	3.07 (0.08)	1.22
6	0.14 (0.30)	1.66 (0.47)	2.85 (0.23)	1.48
	450−550 Emission at 70 °C			
4	0.08 (0.76)	0.52 (0.22)	2.16 (0.02)	0.22
5	0.32 (0.75)	2.09 (0.25)		0.77
6	0.24 (0.72)	0.82 (0.24)	2.56 (0.04)	0.46
	410−425 Emission at 70 °C			
4	0.09 (0.64)	0.59 (0.32)	1.96 (0.04)	0.32
5	0.46 (0.20)	2.19 (0.80)		1.83
6	0.41 (0.64)	1.17 (0.34)	4.30 (0.02)	0.72

[a] Samples were dissolved in 7.5 mM phosphate buffer at pH 7.0 with 10 μM Na_2EDTA and 1.0 M NaCl. Duplex concentrations were 1.0 ± 0.1 × 10^{-5} M. λ_{exc} was 355 nm; the spectral bandwidth for emission measurements was 8 nm. Samples were held in quartz semi-microcells and excited through the 4-mm-path-length direction. All samples were deoxygenated prior to kinetics measurements by bubbling with N_2 gas for 40 min while stirring. The temperature ranges for the 10 and 70 °C measurements were, respectively, ±0.2 and ±1 °C. [b] (A_i) values in the table are fractional amplitudes for emission lifetime components. Emission decay lifetimes are fit to $f(t) = \sum_{i=1}^{n} A_i\, e^{-t/\tau_i}$, where n = 2 or 3. Residuals in the fits generally range from 2 to 7, and reduced χ^2 values for the fits generally range from 1 to 4. Emission lifetime component and amplitudes are averaged over the indicated wavelength ranges, except where otherwise noted. [c] Average lifetime, $\langle\tau\rangle = \sum_{i=1}^{n} A_i\tau_i$, where n = 2 or 3. Errors in average lifetime values are ±0.15 ns for lifetimes ≥1.1 ns and ±0.10 ns for lifetimes ≤0.8 ns.

DNA Single-Strand Concentration Determination. Complementary single-strand concentrations were calculated based their on room-temperature absorbance at 260 nm using the Warshaw−Tinoco equation.[39] U^{PY}-substituted single-strand concentrations were also based on their room-temperature absorbance but in the ethynylpyrenyl region from 330 to 440 nm. In this region, only the ethynylpyrenyl chromophore absorbs. However, this chromophore's peak positions, molar absorbance values, and bandwidths can vary with changes in the solvent or the DNA strand sequence. We assumed, therefore, that the integrated molar absorbance for the $^1(\pi,\pi^*)$ ethynylpyrenyl electronic transition in this region was the same for the PYdU nucleoside in MeOH as for the U^{PY}-substituted DNA single strands and duplexes in buffer. This yielded a molar absorbance at for 401 nm (ϵ_{401}) of 53(±1) × 10^3 M^{-1} cm^{-1} for duplexes **1**−**5** and a ϵ_{398} of 46(±1) × 10^3 M^{-1} cm^{-1} for duplex **6**.

DNA Duplex Concentration Determination. Duplex solutions were made by combining a known number of moles of a U^{PY}-substituted strand with a 5% molar-equivalent excess of its complementary strand in Milli-Q deionized water. Duplex samples for T_m, CD, absorbance, fluorescence, fluorescence quantum yield, and emission kinetics measurements were made by diluting small volumes of concentrated stock solutions with much larger volumes of our standard buffer solution (7.5 mM phosphate buffer at pH 7.0 with 10 μM Na_2EDTA and 1.0 M NaCl). Duplex concentrations were determined from integration of the ethynylpyrenyl absorbance from 330 to 440 nm and application of Beer's law using the $\epsilon_{330-440}$ value for the PYdU nucleoside in MeOH. Importantly, CD spectral measurements showed that ethynylpyrenyl chromophores of U^{PY}-substituted DNA duplexes did not intercalate into duplex base stacks, as

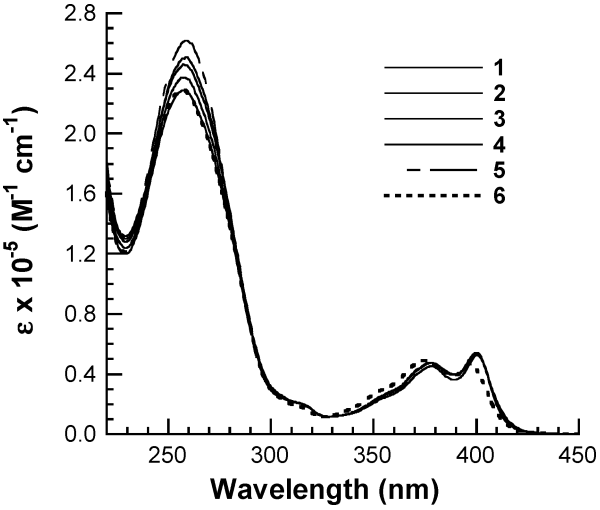

Figure 1. Molar absorbance (ϵ) spectra of six DNA duplexes recorded at room temperature in deoxygenated 7.5 mM phosphate buffer at pH 7.0 with 10 μM Na_2EDTA and 1.0 M NaCl. The spectra of duplexes **1**−**4** are nearly the same; thus they are all plotted with a solid line. ϵ_{259} values for each duplex are given in Table 1.

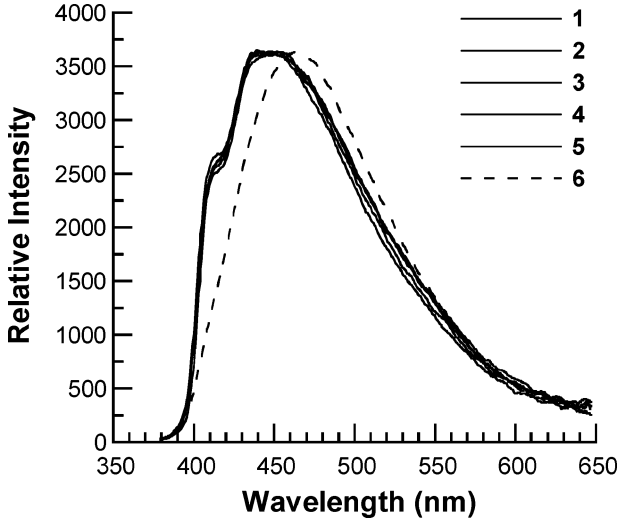

Figure 2. Relative emission spectra (normalized at λ_{max}) for the six DNA duplexes recorded at 10.0 ± 0.2 °C in deoxygenated 7.5 mM phosphate buffer at pH 7.0 with 10 μM Na_2EDTA and 1.0 M NaCl. The spectra of duplexes **1**−**5** are the same; thus they are all plotted with a solid line. The sample concentration range was 7.3−8.4 × 10^{-7} M; λ_{exc} was 365 nm with excitation and emission spectral bandwidths of, respectively, 4 and 2 nm.

no CD absorbance was seen for them between 330 and 440 nm (Figure 1S of the Supporting Information).

Results and Discussion

DNA Strand Sequences. Chart 1 presents structural drawings of the U^{PY} and U^{F} C5-substituted 2′-deoxyuridine nucleotides that, respectively, functioned as a source of a photoinduced excess electron and as a trap for such an electron in the DNA duplexes in this study. Table 1 presents the base sequences of the U^{PY}-substituted DNA strands synthesized in this work to make duplexes **1**−**6**. Duplexes **1**−**4** have the same 5′-AAAGG-3′ base sequence in the 3′-direction away from an internal U^{PY} nucleotide and also have the same complementary strand. They differ in the 5′-direction away from U^{PY} in the number of T nucleotides separating the U^{PY} electron source and the U^{F} electron trap: 0 to 3, respectively, for duplexes **1**−**4**. Duplex **5** has a central U^{PY} nucleotide and same-strand, nearest-neighbor AA pairs. This duplex, therefore, does not permit facile, same-strand, excess electron hopping in either direction away from U^{PY}, as an A nucleotide is much harder to reduce than either U or T nucleotides. Duplex **6** also has a central U^{PY} nucleotide but with same-strand, nearest-neighbor TT pairs. This duplex, therefore, does permit excess electron hopping in either direction away from U^{PY}. Note also that the asymmetry of flanking bases on either side of U^{PY} in the **1**−**4** series of duplexes means that same-strand, excess electron hopping in the 3′-direction away from U^{PY} is thermodynamically uphill. Rather, in these four duplexes, same-strand electron hopping away from U^{PY} in the 5′-direction is much preferred over that in the 3′-direction. Of course, if the excess electron in the $PY^{\bullet+}/dU^{\bullet-}$ CT excited state within U^{PY} were restrained from hopping to nearby U^{F} traps due to attraction to $PY^{\bullet+}$, the CT excited-state dynamics within the **1**−**4** series of duplexes would be much the same.

Duplex Molar Absorbance (ϵ) and Melting Temperature (T_m). Table 1 lists the molar absorbance at 259 nm (ϵ_{259}) and the melting temperature (T_m) for the six duplexes studied here. The average ϵ_{259} for all six duplexes is 2.4 × 10^5 M^{-1} cm^{-1} with less than a 10% deviation from the average for any of them. Figure 1 presents overlayed plots of molar absorbance spectra for three of these duplexes over the 220−450 nm range. The absorbance spectra of duplexes **1**−**4** are so similar that they are all plotted with a solid line. Duplex **5** has the largest ϵ_{259} value but the same molar absorbance values as duplexes **1**−**4** in the 330−440 nm region. Duplex **6** has a slightly blue-shifted pyrenyl band with an absorbance maximum at 398 nm compared to 401 nm for the other five duplexes. Figure 1S of the Supporting Information shows that duplexes **1**−**4** have nearly identical CD spectra in the 220−450 nm region. The CD spectra for duplexes **5** and **6** have weaker absorbance bands than do the spectra for the other four duplexes. Despite some CD absorbance differences, the T_m values of duplexes **1**−**4** and **6** are all 40 °C. Duplex **5** has the lowest T_m at 37 °C, but duplex **6** has the weakest CD absorbance bands. Thus, duplexes **1**−**4** appear to have very similar structures, while duplexes **5** and **6** appear to have similar stabilities to duplexes **1**−**4** but somewhat different exciton interactions due to differing base sequences. Inspection of the melting curves for these six duplexes showed that melting did not begin before 10 °C and finished by 70 °C. CD, fluorescence spectroscopy, fluorescence quantum yield, and emission kinetics measurements on the duplexes were carried out at 10.0 ± 0.2 °C. For experimental convenience and because duplex melting was still negligible at room temperature, absorbance spectra were recorded at room temperature. Additionally, emission kinetics measurements of three melted DNA duplexes were carried out at 70 ± 1 °C.

Emission Spectra and Quantum Yields. Figure 2 presents normalized, relative emission spectra for duplexes **1**−**6** at 10 °C. The spectral shapes for duplexes **1**−**5** are identical with emission maxima at ca. 448 nm. The emission spectrum of **6**, however, is red-shifted with a maximum at 464 nm. Thus, both the absorbance and the emission spectra of duplex **6** indicate that the local environment surrounding the pyrenyl chromophore in U^{PY} is somewhat different than those of the other five duplexes. The base sequence of **6** is unique among the six duplexes in that it has a pair of same-strand Ts flanking U^{PY} in the 3′-direction, while all five other duplexes have a pair of As in this position. This change in 3′-bases flanking U^{PY} appears to be responsible for the change in absorbance and emission spectra for **6** compared to the other five duplexes. Table 1 also presents emission quantum yields for the six duplexes in this study. Importantly, duplexes **1**−**5** have the same emission

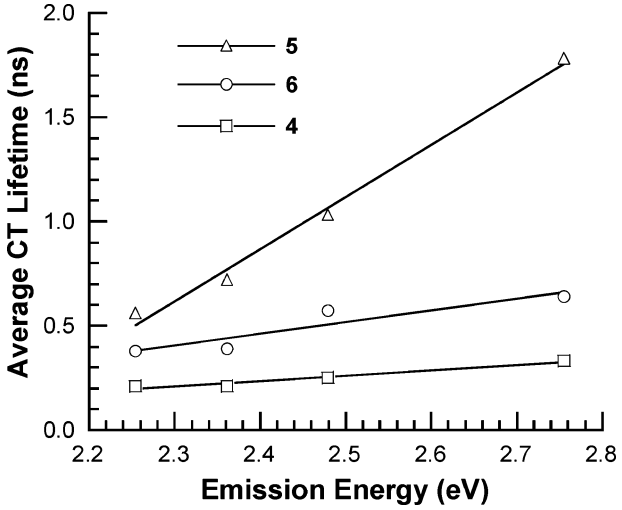

Figure 3. Overlayed plots of average CT emission lifetime versus energy (450−550 nm) for duplexes **4**−**6** at 70 °C. The experimental conditions are the same as those described in Table 2. The solid lines are linear least squares fits to the data. Linear correlation coefficients (*R*) for these fits are, respectively, 0.99, 1.00, and 0.93 for duplexes **4**−**6**.

quantum yield, 0.019 ± 0.003. Duplex **6** again is different with a higher emission quantum yield than the other five duplexes, 0.032. A final comment on the emission spectra in Figure 2 is that pyrenyl emission features are absent for all six duplexes. In U^{PE}-substituted HPs, by contrast, strong pyrenyl features are found for the two HPs lacking U^{X} traps and having a same-strand AA pair flanking U^{PE} in the 3′-direction. Additionally, all of the other seven U^{PE}-substituted HPs studied show weak to moderate pyrenyl features.[25] Sharp ethynylpyrenyl vibrational features are also present in the emission spectrum of the PYdU nucleoside in tetrahydrofuran, MeCN, and MeOH, although mixed with a broad CT emission.[40] Thus, $^1(\pi,\pi^*)$ ethynylpyrenyl emission is sufficiently quenched in the conformations of the U^{PY} nucleotide in the duplexes in this study such that their emission spectra are due solely to their $PY^{\bullet+}/dU^{\bullet-}$ CT state.

Emission Lifetimes. Table 1S of the Supporting Information presents exponential lifetime fits to emission decay at nine wavelengths from 410 to 600 nm at 10 °C for duplexes **1**−**6** and at six wavelengths from 410 to 550 nm at 70 °C for duplexes **4**−**6**. All of the emission kinetics for all duplexes at 10 °C require three exponential lifetimes for best fitting. At 70 °C, kinetics fits for duplexes **4** and **6** require three lifetimes, but fits for **5** require only two lifetimes. At 10 °C for a given duplex, there are no clearly discernible differences among corresponding lifetime components and amplitudes at different wavelengths. Thus, at 10 °C, Table 2 reports lifetime components (τ_i) and amplitudes (A_i) averaged over all nine wavelengths ($\langle\tau_i\rangle$ and $\langle A_i\rangle$) as well as the resulting average CT emission lifetime ($\langle\tau\rangle$) for each duplex.

At 70 °C where duplexes **4**−**6** are melted, a clear pattern of decreasing lifetime with increasing wavelength is present for duplex **5** in the CT region from 450 to 550 nm. Figure 3 plots these data as the average CT lifetime versus the emission energy for all three duplexes studied at 70 °C. As shown in Figure 3, the slope of the linear correlation of average CT lifetime versus emission energy is steep for duplex **5**, is less steep for **6**, and approaches zero for **4**. In fact, wavelength-dependent average CT lifetime behavior is significant only for duplex **5** at 70 °C among all of the duplexes studied here at both 10 and 70 °C. In contrast, a previous study of U^{PE}-substituted HPs at room temperature found such wavelength-dependent CT lifetime behavior prominent for eight out of nine HPs studied (both with and without U^{X} traps).[25] The key difference between the U^{PY} duplexes here and prior U^{PE} HP studies appears to be that the linker joining pyrene to dU is rigid in U^{PY} (ethyne) and flexible in U^{PE} (ethylene). Earlier wavelength-dependent average CT lifetime behavior was ascribed to multiple conformations of the U^{PE} nucleotide in DNA HPs.[25] This earlier assignment is supported by the finding here that the average CT lifetime is independent of wavelength at 10 °C for all six U^{PY}-substituted duplexes and is clearly found only once (i.e., when duplex **5** is melted). To compare duplexes **4**−**6** at 70 °C on the same basis, Table 2 reports the lifetime components and amplitudes for these three duplexes averaged separately over the 410−425 and 450−550 nm ranges. Average emission lifetimes in each range ($\langle\tau\rangle$) are also given.

The most important results in Table 2 deal with the average CT lifetimes ($\langle\tau\rangle$) at 10 °C and their relationship to the emission quantum yields discussed above. A second point of interest deals with the effect that melting duplexes **4**−**6** has on their excited-state dynamics. Table 2 shows that duplexes **1**−**5** at 10 °C have an average $\langle\tau\rangle$ (average CT lifetime) of 1.22 ns (σ = 0.10 ns); that is, these CT lifetimes are the same independent of where the U^{F} trap is located or even whether or not a U^{F} trap is present. This result also accords with the earlier finding that duplexes **1**−**5** had the same emission quantum yield of 0.019 ± 0.003. Duplex **6** has both a higher emission quantum yield (0.032) and a higher average CT lifetime (1.48 ns) than those of duplexes **1**−**5**. However, within error, the quantum yield increase is consistent with the average CT emission lifetime increase. Thus, the CT lifetime and emission quantum yield data for duplexes **1**−**6** at 10 °C are in accord.

U^{PY}-substituted duplexes, where enhanced CT emission quantum yield (i.e., a quantum yield above that expected due to increased average CT lifetime) is lacking for duplexes with U^{F} electron traps compared to duplexes without traps, contrast strongly with U^{PE}-substituted HPs where up to 4.5-fold enhanced CT emission quantum yield is found for HPs with U^{Br} and U^{F} traps compared to HPs without traps.[25] The earlier paper ascribed the enhanced CT emission quantum yield in the presence of U^{X} electron traps to type 2 CS between the pyrenyl excited state of U^{PE} and a trap to form $PE^{\bullet+}/U^{X\bullet-}$ products that decayed to form the emissive $PE^{\bullet+}/dU^{\bullet-}$ CT state of U^{PE}. Key to this pyrenyl oxidative quenching process was the flexible ethylenyl linker in U^{PE}. The observation here for duplexes at 10 °C that there is no enhancement of CT emission quantum yield when U^{F} electron traps are located near U^{PY} is consistent with the earlier U^{PE}-substituted HP work, because the rigid ethynyl linker in U^{PY} is not expected to permit pyrenyl oxidative quenching by such traps.

Melting duplexes **4**−**6** shortens all of their average CT lifetimes: for **4** from 1.37 to 0.22 ns, for **5** from 1.22 to 0.77 ns, and for **6** from 1.48 to 0.46 ns. It is difficult to be sure why these CT lifetimes shorten upon duplex melting, but the data suggest that neighboring same-strand bases play an important role. The greatest CT lifetime shortening occurs for duplex **4** with four same-strand pyrimidines and a U^{F} trap on the 5′-side of U^{PY}; perhaps as a single strand at 70 °C, the U^{F} trap can "short-circuit" the $PY^{\bullet+}/dU^{\bullet-}$ CT state of U^{PY} via formation of a $U^{F\bullet-}$ intermediate. The least CT lifetime shortening occurs for duplex **5** in which U^{PY} does not have same-strand primidine nearest or next-nearest neighbors. In this case at 70 °C, the flanking AA pairs on each side of U^{PY} cannot provide a short-circuit route as U^{F} can in duplex **4**. Duplex **6** has same-strand TT pairs on either side of U^{PY}, and at 70 °C these can short-

circuit the CT state of U^{PY} via formation on a $T^{\bullet-}$ intermediate. However, this intermediate is less easily formed than $U^{F\bullet-}$. Thus, CT lifetime shortening upon duplex melting for **6** (with flanking Ts) that is intermediate between that observed for **4** (with a flanking U^F) and that observed for **5** (with flanking As) is consistent with enhanced short-circuit CT quenching at 70 °C compared to 10 °C, as the reduction potential for T is intermediate between those for U^F and A. While the dominant decay pathway for the CT state of U^{PY} in duplexes **4** and **6** at 70 °C is likely to be short-circuit quenching by nearest-neighbor pyrimidines, this is less certain for duplex **5** whose nearest pyrimidines are three bases away from U^{PY}. The presence of a small amount of across-strand ET to nearby Ts from the CT state of U^{PY} in **5** cannot be ruled out as contributing to the longer CT state lifetime of **5** at 10 °C compared to that at 70 °C. Loss of such across-strand ET in **5** due to melting could also contribute to shortening the lifetime of the CT state of U^{PY} in **5**.

The average lifetimes of the dual pyrenyl/CT emission for duplexes **5** and **6** at 70 °C are worth pointing out, respectively, 1.83 and 0.72 ns. These emission lifetimes can be compared with the corresponding average lifetimes at 10 °C, respectively, 1.22 and 1.48 ns. Melting duplex **5** removes across-strand TT pairs from either side of U^{PY} in the duplex form and leaves it in an oligomer with same-strand flanking AA pairs. The consequence is an increased average lifetime for pyrenyl emission at 70 °C compared to that at 10 °C. In contrast, melting duplex **6** leaves U^{PY} in an oligomer with same-strand flanking TT pairs on either side. The consequence is a decreased average lifetime for pyrenyl emission at 70 °C compared to that at 10 °C.

Conclusions

The U^{PY}-substituted DNA duplexes in this work test and support the conclusions reported by Gaballah et al.[25] based on U^{PE}-substituted DNA HPs. In their model, the pyrenyl excited state of U^{PE} reduced a U^X trap to form a $PE^{\bullet+}/U^{X\bullet-}$ product (type 2 CS) that decayed to form the emissive $PE^{\bullet+}/dU^{\bullet-}$ CT state of U^{PE}. This process produced enhanced CT emission quantum yields for HPs with U^X electron traps compared to HPs without traps. As expected because of the rigid ethynyl linker in U^{PY} (compared to the ethylenyl linker in U^{PE}), U^{PY}-substituted duplexes lack most of the type 2 CS found in the earlier HP study. Thus, in U^{PY}-substituted duplexes, enhanced CT emission quantum yields are not found for duplexes with U^F electron traps near U^{PY} compared to duplexes without traps. Furthermore, the average CT lifetime and emission quantum yield of U^{PY}-substituted duplexes are independent of U^F trap location. These new results strongly suggest that the excess electron in the $PY^{\bullet+}/dU^{\bullet-}$ CT product of U^{PY} is restrained from hopping to nearby U^F traps due to attraction to $PY^{\bullet+}$. This conclusion is reasonable in view of the Coulombic attraction between the cation and anion subunits of the CT state of U^{PY}.

Acknowledgment. We thank the donors of the Petroleum Research Fund, administered by the ACS, for support of this research.

Supporting Information Available: CD spectra for all HPs, emission quantum yield methods, emission lifetime methods, oligomer purification and desalting, DNA duplex concentration determination, and duplex emission kinetics at individual wavelengths for all HPs. This material is available free of charge via the Internet at http://pubs.acs.org.

References and Notes

(1) *Long-Range Electron Transfer in DNA I*; Schuster, G. B., Ed.; Topics in Current Chemistry 236; Springer-Verlag: Berlin, 2004.
(2) *Long-Range Electron Transfer in DNA II*; Schuster, G. B., Ed.; Topics in Current Chemistry 237; Springer-Verlag: Berlin, 2004.
(3) Steenken, S. *Chem. Rev.* **1989**, *89*, 503−520.
(4) Steenken, S.; Telo, J. P.; Novais, H. M.; Candeis, L. P. *J. Am. Chem. Soc.* **1992**, *114*, 4701−4709.
(5) Steenken, S. *Free Radical Res. Commun.* **1992**, *16*, 349−379.
(6) Razskazovskii, Y.; Swarts, S. G.; Falcone, J. M.; Taylor, C.; Sevilla, M. D. *J. Phys. Chem. B* **1997**, *101*, 1460−1467.
(7) Messer, A.; Carpenter, K.; Forzley, K.; Buchanan, J.; Yang, S.; Razskazovskii, Y.; Cai, Z.; Sevilla, M. D. *J. Phys. Chem. B* **2000**, *104*, 1128−1136.
(8) Cai, Z.; Xifeng, L.; Sevilla, M. D. *J. Phys. Chem. B* **2002**, *106*, 2755−2762.
(9) Giese, B.; Carl, B.; Carl, T.; Carell, T.; Behrens, C.; Hennecke, U.; Shiemann, O.; Feresin, E. *Angew. Chem.* **2004**, *116*, 1884−1887.
(10) Ito, T.; Rokita, S. E. *Angew. Chem., Int. Ed.* **2004**, *43*, 1839−1842.
(11) Breeger, S.; Hennecke, U.; Carell, T. *J. Am. Chem. Soc.* **2004**, *126*, 1302−1303.
(12) Haas, C.; Kraling, K.; Cichon, M. K.; Rahe, N.; Carell, T. *Angew. Chem.* **2004**, *116*, 1878−1880.
(13) Behrens, C.; Burgdorf, L. T.; Schwogler, A.; Carell, T. *Angew. Chem., Int. Ed.* **2002**, *41*, 1763−1766.
(14) Cichon, M. K.; Haas, C.; Grolle, F.; Mees, A.; Carell, T. *J. Am. Chem. Soc.* **2002**, *124*, 13984−13985.
(15) Schwogler, A.; Burgdorf, L. T.; Carell, T. *Angew. Chem., Int. Ed.* **2000**, *39*, 3918−3920.
(16) Behrens, C.; Cichon, M. K.; Grolle, F.; Hennecke, U.; Carell, T. In *Long-Range Electron Transfer in DNA I*; Schuster, G. B., Ed.; Topics in Current Chemistry 236; Springer-Verlag: Berlin, 2004; pp 187−204.
(17) Lewis, F. D.; Liu, X.; Wu, Y.; Miller, S. E.; Wasielewski, M. R.; Letsinger, R. L.; Sanishvili, R.; Joacimiak, A.; Tereshko, V.; Egli, M. *J. Am. Chem. Soc.* **1999**, *121*, 9905−9906.
(18) Lewis, F. D.; Liu, X.; Miller, S. E.; Hayes, R. T.; Wasielewski, M. R. *J. Am. Chem. Soc.* **2002**, *124*, 11280−11281.
(19) Lewis, F. D.; Wu, Y.; Liu, X. *J. Am. Chem. Soc.* **2002**, *124*, 12165−12173.
(20) Ito, T.; Rokita, S. E. *J. Am. Chem. Soc.* **2003**, *125*, 11480−11481.
(21) Wagenknecht, H.-A. *Curr. Org. Chem.* **2004**, *8*, 251−266.
(22) Rist, M.; Amann, N.; Wagenknecht, H.-A. *Eur. J. Org. Chem.* **2003**, 2498−2504.
(23) Amann, N.; Pandurski, E.; Fiebig, T.; Wagenknecht, H.-A. *Angew. Chem., Int. Ed.* **2002**, *41*, 2978−2980.
(24) Amann, N.; Pandurski, E.; Fiebig, T.; Wagenknecht, H.-A. *Chem.—Eur. J.* **2002**, *8*, 4877−4883.
(25) Gaballah, S. T.; Vaught, J. D.; Eaton, B. E.; Netzel, T. L. *J. Phys. Chem. B* **2005**, *109*, 5927−5934.
(26) Kerr, C. E.; Mitchell, C. D.; Headrick, J.; Eaton, B. E.; Netzel, T. L. *J. Phys. Chem. B* **2000**, *104*, 1637−1650.
(27) Kerr, C. E.; Mitchell, C. D.; Ying, Y.-M.; Eaton, B. E.; Netzel, T. L. *J. Phys. Chem. B* **2000**, *104*, 2166−2175.
(28) Mitchell, C. D.; Netzel, T. L. *J. Phys. Chem. B* **2000**, *104*, 125−136.
(29) Raytchev, M.; Mayer, E.; Amann, N.; Wagenknecht, H.-A.; Fiebig, T. *ChemPhysChem* **2004**, *5*, 706−712.
(30) Netzel, T. L.; Nafisi, K.; Headrick, J.; Eaton, B. E. *J. Phys. Chem.* **1995**, *99*, 17948−17955.
(31) Netzel, T. L.; Zhao, M.; Nafisi, K.; Headrick, J.; Sigman, M. S.; Eaton, B. E. *J. Am. Chem. Soc.* **1995**, *117*, 9119−9128.
(32) Korshun, V. A.; Manasova, E. V.; Balakin, K. V.; Prokhorenko, I. A.; Buchatskii, A. G.; Berlin, Y. A. *Russ. J. Bioorg. Chem.* **1996**, *22*, 807−809.
(33) This study of U^{PY}-substituted DNA uses duplex structures. While HP structures are perhaps easier to handle and show concentration-independent melting temperatures, they are generally purified via HPLC with a column heated to ca. 60 °C to melt the HPs. However, since only FPLC purification equipment was available for this study and the FPLC column could not be heated, we elected to work with duplexes whose constituent oligomers could be purified at room temperature.
(34) Eckstein, J. W.; Hastings, J. W.; Ghisla, S. *Biochemistry* **1993**, *32*, 404−411.
(35) Detailed comparison of the photophysical and photochemical CS processes in the PYdU and PEdU nucleosides is sufficiently complicated and interesting that the subject warrants treatment in a separate paper. Such a paper will be forthcoming. However, one might reasonably guess that CS within the former nucleoside would be much faster than in the latter. If so, both the rigidity of the ethynyl linker in PYdU and its much faster photoinduced CS would be responsible for the elimination of most of the type 2 CS found in the earlier study of U^{PE}-substituted HPs. In fact both PYdU and PEdU have multiple conformations in solution, and their CS

reactions, as evidenced by their pyrenyl $^1(\pi,\pi^*)$ emission kinetics, exhibit multiple lifetimes. The longest pyrenyl emission lifetime components for the PYdU and PEdU nucleosides in MeOH are, respectively, 34 and 75 ns. Most conformers of both nuclesides, however, appear to undergo photo-induced CS in less than 0.1 ns (the resolution limit of our emission kinetics equipment) as rise times for CT state emission are never seen. Furthermore, picosecond transient absorbance measurements of PEdU in MeOH show that the majority of the absorbance of the CT state forms in less than 30 ps, again, as no rise time is seen. Thus, while the fastest reacting conformers of PYdU may undergo CS much faster than the corresponding conformers of PEdU, it appears that both would then do so in less than 30 ps. In MeOH, pyrenyl emission is much less prominent for PYdU than that for PEdU, suggesting that in this solvent the fraction of conformers that undergo slow CS is much smaller in the former than in the latter nucleoside. In DNA duplexes and HPs substituted with U^{PY} and U^{PE}, however, there is no a priori way of guessing the distribution of pyrene−dU conformers. Current work at GSU is developing new AMBER force field parameters so that molec-
ular dynamics computations will be able to address such questions in the future.

(36) Lakowicz, J. R. *Principles of Fluorescence Spectroscopy*; Plenum Press: New York, 1986; p 496.

(37) Creutz, C.; Chou, M.; Netzel, T. L.; Okumura, M.; Sutin, N. *J. Am. Chem. Soc.* **1980**, *102*, 1309−1319.

(38) Duncan, D. C.; Netzel, T. L.; Hill, C. L. *Inorg. Chem.* **1995**, *34*, 4640−4646.

(39) Warshaw, M. M.; Tinoco, I., Jr. *J. Mol. Biol.* **1966**, *20*, 29−38.

(40) Hussein, Y. H. A.; Gaballah, S. T.; Netzel, T. L., to be submitted for publication.